

Highly Collimated Photon Detection using Strongly Coupled Superconducting Tunnel Junctions

N.Rando, C.L. Foden, A.Peacock, A. van Dordrecht
Astrophysics Division, Space Science Department of the European Space Agency,
ESTEC, Noordwijk, The Netherlands.

J.Lumley, C.Pereira
Oxford Instruments Scientific Research Division, Cambridge, UK.

Abstract . Preliminary results on the X-Ray performance of Nb based superconducting tunnel junctions (STJ's) with a highly transmissive barrier are reported. The results of the investigation show that the energy resolution of these detectors can be improved by collimating the X-Ray photons onto the junction barrier area, thus reducing illumination of the surrounding substrate and leads. A charge output of about 50% of the theoretical maximum has been recorded for these STJ's, with a FWHM resolution of about 200 eV at 6 KeV. Several mechanisms which are believed to degrade the energy resolution are also discussed. X-Ray events are also detected by other junctions on the same chip which are not illuminated. This may indicate the presence of a marked phonon transmission along the sapphire substrate which acts as a "Phonon Wave-Guide", analogous to the light transmission mechanism in fibre optics.

I. INTRODUCTION.

The absorption of high energy photons in matter produces, according to a relaxation process defined by the radiation wavelength and by the characteristics of the absorbing material, a number of charge carriers. The total number of carriers and its variance at the end of this relaxation process define the intrinsic energy resolution of any detector based on the photoabsorption mechanism.

Superconductors offer important advantages over semiconductors for the development of high resolution photon spectrometers: firstly the small energy gap 2Δ , generally thousand times smaller than the one of a semiconductor based detector, and secondly the fact that the Debye energy (of order 10's meV) is greater than the energy gap (of order meV).

The size of the energy gap ($2\Delta = 3.1$ meV in Niobium) means that the total number of carriers produced by photoabsorption in a superconductor is about thousand times higher than in a semiconductor ($E_g = 1.1$ eV in Silicon), such that the statistical fluctuation on this charge is proportionally reduced [1].

As a result of the Debye and gap energies the relaxation processes occurring after the photoabsorption are dominated by a close interaction between quasi-particle and phonon populations [2], [3]; phonons with an energy $> 2\Delta$ can still contribute to increasing quasi-particle population through the breaking of Cooper pairs. In semiconductors $\Omega_d < E_g$ and therefore there can not be any major coupling between the two

populations such that any phonon produced during the relaxation process represents an energy loss in the system, therefore reducing the final quantum efficiency of the detector.

The number of quasiparticles N_0 produced by a photon of energy E_p can be written as $N_0 = E_p/\epsilon$, where ϵ is the energy required to create a single carrier. In niobium, the theoretical value for ϵ is equal to 1.747Δ [1]. Assuming that all this charge can be extracted from the superconductor by quasiparticle tunneling across the junction barrier, then the intrinsic energy resolution of the detector would be given by $R_0(\text{eV}) = 2.355(F\epsilon E_p)^{1/2}$, where F is the Fano factor [1], (F has been calculated to be 0.22 for niobium). For a 6 KeV X-Ray photon these values give $N_0 = 2.2 \times 10^6$ and $R_0(\text{eV}) = 4$ eV (FWHM). This Fano limited resolution has never been achieved in STJ's due to a multitude of effects which degrade the detector performance; namely phonon loss from the thin films, quasiparticle recombination and diffusion out of the tunneling region, barrier nonuniformities as well as spatially dependent variations in the energy gap.

In this paper, preliminary results of the effects on the detector performance of limiting the X-Ray illumination only to the actual junction area are presented. The utilisation of a highly collimating mask (20 μm diameter) has allowed testing of a junction's spectroscopic performance by reducing the contribution from the surrounding substrate region and the superconducting leads.

II. THE STJ's CHARACTERISTICS.

The junctions have been fabricated from an original trilayer (Nb-Al-AlOx-Nb) deposited on a highly polished sapphire substrate 0.5 mm thick: the first Nb layer (500 Angstrom thick) was grown epitaxially on the sapphire, while the top layer (850 Angstrom thick, deposited onto the thin AlOx film) is polycrystalline. The Al film thickness is estimated to be 40 Angstrom, while both capacitance measurements and a multiple particle tunnelling model indicate an AlOx thickness of less than 10 Angstrom [2]. Each chip contains 8 junctions (four $12 \times 12 \mu\text{m}$, three $20 \times 20 \mu\text{m}$ and one $50 \times 50 \mu\text{m}$): the results reported in this paper refer to a $20 \times 20 \mu\text{m}$ junction (on which the mask was aligned, see Fig.1) and to a $12 \times 12 \mu\text{m}$ (not illuminated by X-Rays). SEM inspections of similar chips, showed a significant improvement over previous chips [1] in the photolithographic procedure, with a much better defined junction and lead geometry (the width of the electrical leads is 5 μm). Further detail on the fabrication procedure of these junctions can be found in references [1], [4] and [5]. Their I-V characteristics have been extensively investigated in [4]. The current - temperature variation of the $20 \times 20 \mu\text{m}$ device was found to

The authors wish to acknowledge the support given by W.Fischer and J.van der Biezen of the Astrophysics Division for the alignment of the mask on the selected detector.

Manuscript received August 24, 1992.

follow the predicted BCS model with an additional leakage current of $0.05 \text{ nA}/\mu\text{m}^2$.

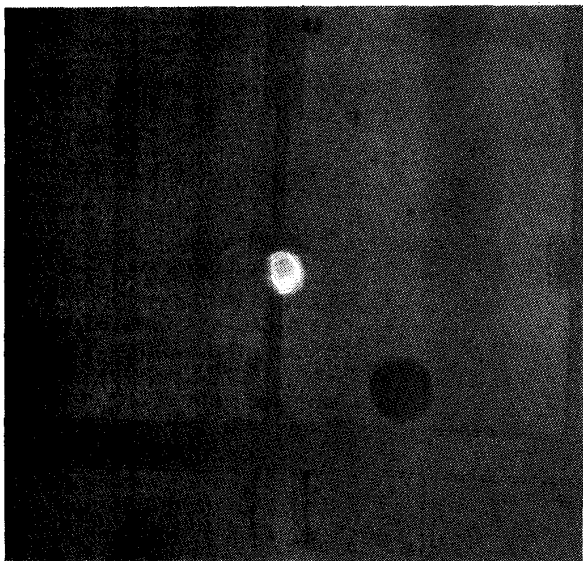


Fig.1 Mask alignment: the white spot indicates the collimating hole position with respect to the $20 \times 20 \mu\text{m}$ device.

The barrier uniformity has been clearly demonstrated by the measurement of the Josephson critical current as function of the applied magnetic field. The electrical characteristics of the devices are given in Table 1: I_{th} is the thermal current measured at a bias voltage of 0.5 mV and at 1.2 K ; the other parameters were measured at 4.2 K . It is important to note that the junction design has been optimised for a short confinement time by reducing the film thicknesses and the normal resistance R_n [6]. Confinement times τ_c of 110 nS (top film) and 65 nS (bottom film) for the $20 \times 20 \mu\text{m}$ junction have been achieved. Since quasiparticle tunnelling occurs in competition with recombination and diffusion out of the tunnel region, τ_c must be minimised to increase the detected charge N . As a result of this optimisation, the charge output has increased up to the 55 % of the theoretically predicted value, the highest achieved to date with Nb based STJ's. Since R_n is so low (0.6 ohm), the Josephson critical current is now difficult to suppress using low magnetic fields at the minima of the Fraunhofer pattern. The high magnetic field necessary for suppression causes a shift in Δ from about 1.48 meV ($B = 0$) to 1.43 meV ($B = 600 \text{ Gauss}$), in addition to smearing the sharp edge of the energy gap.

This magnetic field dependence of the gap is probably responsible for a further degradation of the energy resolution [6].

Table 1 Junctions properties.

STJ(μm)	$R_n(\Omega)$	$V_g(\text{mV})$	$I_c(\text{mA})$	$I_{th}(\text{nA})$
20x20	0.6	2.96	2.3	15.9
12x12	1.6	2.96	1.1	1.5

III. EXPERIMENTAL RESULTS.

The X-Ray performance of the $20 \times 20 \mu\text{m}$ STJ has been investigated using a 50mCi Fe^{55} source, emitting two line complexes from $\text{Mn K}\alpha$ (mean energy 5895 eV) and from $\text{Mn K}\beta$ (mean energy 6401 eV), with an intensity ratio of 8.4. A detailed description of the experimental set-up has been given elsewhere [1], [2]. The use of a metallic collimating mask (collimating aperture diameter = $20 \mu\text{m}$), positioned as close as possible to the STJ surface (distance $< 100 \mu\text{m}$) in order to minimise the beam spread, allows illumination of a single $20 \times 20 \mu\text{m}$ junction, as shown in Fig.1. All the other STJ's on the chip were not illuminated by X-rays, therefore any feature recorded in their energy spectrum could only be due to indirect detection, i.e. a substrate event followed by phonon transmission along the substrate or quasiparticle diffusion along the connecting wires into the device from events absorbed in the device under illumination. The electronic noise of the system is well known and falls below the lower level discriminator. The presence of such a small collimating hole has seriously reduced the count rate during the spectrum acquisition, such that very long runs are necessary. The spectrum shown in Fig.2(a) corresponds to a continuous acquisition of 24 hours, during which the biasing conditions were kept as constant as possible ($T = 1.21 \text{ K}$, $B = 1050 \text{ Gauss}$, $V_b = 0.25 \text{ mV}$). The stability of the system has been also confirmed by the separate analysis of data blocks acquired at different times.

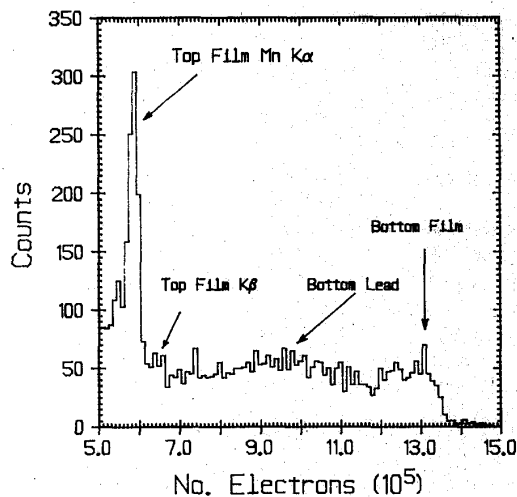


Fig. 2(a) Fe^{55} spectrum obtained in the "masked" configuration with the $20 \times 20 \mu\text{m}$ device.

The spectrum of Fig.2(a) should be compared with the one of Fig.2(b), obtained with the same junction, in similar conditions, but without the collimating mask [6].

In any comparison between these spectra it must be stressed that the mask hole is not perfectly centred on the junction but is offset by about $10\ \mu\text{m}$ in such a way as to directly illuminate the lead of the bottom film (Fig. 1). Furthermore it should be stressed that in the "masked" configuration a special fixture was required, such that the chip to cold finger coupling was weaker than in the "unmasked" configuration [see differences between "damped" and "undamped" configuration discussed in [1].

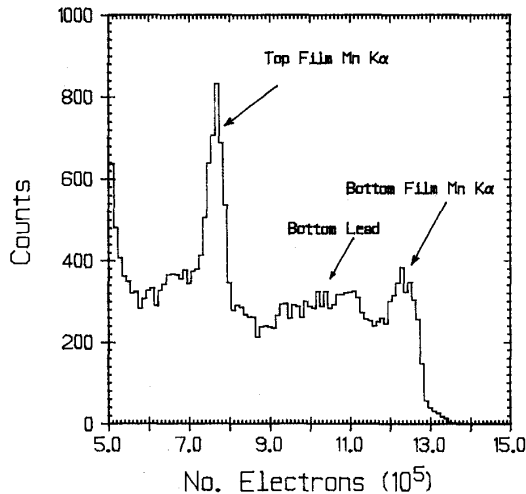


Fig. 2(b) Fe55 spectrum obtained in the "unmasked" configuration with the $20 \times 20\ \mu\text{m}$ device.

Significant differences do, however, still exist between these two spectra. Firstly the discrete line from Mn K_{α} attributable to the top film [6] is about 20 % lower in charge in the masked configuration, while the position of Mn K_{α} from the bottom film remains approximately the same. Secondly, the ratio of the peak intensity of these two components is very different (6 for the masked configuration compared to about 2 for the normal uniform illumination). The latter effect can be explained in terms of different top-bottom film volume ratios: in the masked configuration only part of the lead from the bottom film and part of the bottom film region which is not covered by the barrier (the "underlap" region) are illuminated (Fig. 1). Moreover, part of the top film above the tunnel barrier is illuminated but none of the top lead. This form of illumination causes a worse resolution for the bottom film when masked, but an improved resolution for the top film, i.e. the resolution degradation is clearly related to charge diffusion in and out of leads.

The low energy tail which is visible in Fig. 2(b) at about $5 \times 10^5\ e^-$, is related to phonon induced events generated by photons absorbed in the substrate. This structure, not shown in Fig. 2(a), is also visible in the unmasked configuration.

A preliminary analysis of the spectrum from the top film, involving sets of data accumulated over a 3 day period,

indicates that a considerable structure is present. Although a resolution of below 200 eV was derived, the spectrum was not well fitted by a single gaussian distribution.

A possible explanation for the observed decrease in charge from the top film may also be related to the form of the illumination in the masked configuration in addition to different chip to cold finger coupling conditions and slightly different biasing parameters. Furthermore, run to run charge output variations of this magnitude have been often observed during the tests. In the masked configuration no quasiparticles are created in the connecting niobium regions i.e. ground line and lead (see Fig.1). On the contrary, in the unmasked configuration such events create a source of quasiparticles which can reach the top film, thereby degrading the resolution, yet increasing the charge detected.

In order to understand the role of the phonon propagation in the substrate, an energy spectrum from a non-illuminated $12 \times 12\ \mu\text{m}$ STJ has been acquired: the result (Fig.3) shows that there are no peaks from direct X-Ray detection in the superconducting films, but also that a marked 2 component low energy structure is present, strongly spread in risetime, and certainly due to indirect events followed by phonon propagation within the sapphire.

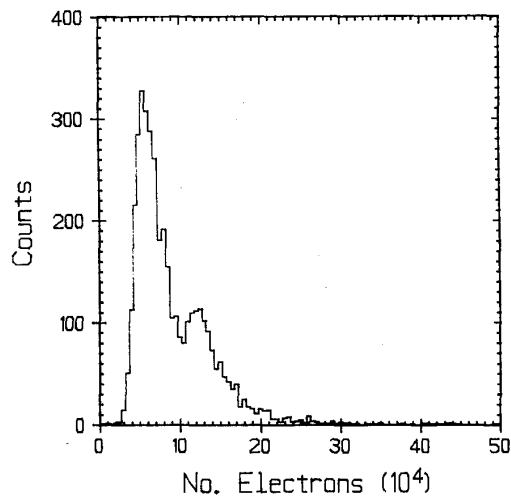


Fig 3 Energy spectrum obtained by a not illuminated $12 \times 12\ \mu\text{m}$ device on the same chip.

The low and high charge components have rather long mean risetimes, of 1.4 and $2.0\ \mu\text{sec}$ respectively. As the phonons propagate, multiple reflection occurs between the opposite substrate surfaces, corresponding to an acoustic wave confinement mechanism possibly similar to the critical reflection or confinement of light in fibre optics. This explains both the spread in risetime, clearly due to the different path lengths of the phonons, each one with a different number of reflections and therefore with a different travel time, and the propagation of the perturbation over considerable distances

(from the 20x20 μm STJ to the 12x12 μm detector there is a direct distance of about 325 μm). The sapphire substrate acts as a "Phonon Wave-Guide" for indirect events. The multiple reflection mechanism will certainly be governed by interface characteristics such as surface finish, presence of other materials (see deposited thin films [7] and cold finger) as well as phonon focusing within the sapphire [8], [9]. The role of the substrate coupling with the cryostat cold finger has been already found to be relevant and it has been studied in a previous paper [1]. The origin of the double component is still, however, unclear. Further investigations are currently being performed to allow a better characterisation of the importance of each of these parameters.

IV. SUMMARY.

The X-Ray performance of a high quality niobium STJ with a highly transmissive barrier has been investigated using a 20 μm diameter collimating mask. The use of the mask, centred approximately on the detector, has allowed the investigation of geometrical effects on the observed energy spectrum as well as reducing the phonon induced pile-up effects due to the simultaneous illumination of different areas surrounding the tunnel region of the junction. This has produced an improvement in the energy resolution of the top film to below 200 eV (FWHM). In addition, X-Ray events absorbed in the substrate directly below the 20 μm device have produced phonons which have been detected indirectly by a device over 300 μm away, indicating that phonon propagation within the substrate can occur over large distances, presumably through a multiple reflection mechanism. Future activities will concentrate on a more precise mask alignment and on a detailed quantitative analysis.

REFERENCES.

- [1] N. Rando, A. Peacock, A. van Dordrecht, C. Foden, R. Engelhardt, B.G. Taylor, P.Gare, J. Lumley, C. Pereira, Nucl. Instrum. & Methods A313, 173 (1992).
- [2] M. Kurakado, H. Mazaki, Nucl. Instrum. & Methods A185, 141 (1981).
- [3] D. Van Vechten, K.S. Wood, Phys. Rev. B, 43, 16, 12852 (1991).
- [4] C.L. Foden, N. Rando, A. van Dordrecht, A. Peacock, J. Lumley, C. Pereira, Submitted to Phys. Rev.B (1992).
- [5] N.Rando, A. Peacock, C. Foden, A. van Dordrecht, R. Engelhardt, J. Lumley, C. Pereira, SPIE Proceedings 1549, 340 (1991).
- [6] N. Rando, A. Peacock, C. Foden, A. van Dordrecht, J. Lumley, C. Pereira, submitted to J. Appl. Phys. (July 1992).
- [7] S.B. Kaplan, J. Low Temp. Phys., 37, 334, (1979).
- [8] R. J. von Gutfeld, A.H. Nethercot, Phys. Rev. Lett., 12, 641 (1964).
- [9] H.J. Marris, Non-equilibrium Phonons in Non-metallic Crystals, (ed. Eisenmenger & Kaplyanskii), 16, 51, (1986).